Available online at www.sciencedirect.com
SCIENCE DIRECT®
Journal of Nuclear Materials 348 (2006) 79–86
journal of nuclear materials
www.elsevier.com/locate/jnucmat

Oxidation of Zircaloy-4 by oxygen and the production of water

N. Stojilovic, E.T. Bender, R.D. Ramsier *

Departments of Physics and Chemistry, The University of Akron, 250 Buchtel Commons, Ayer Hall Room 111, Akron, OH 44325-4001, USA

Received 18 January 2005; accepted 22 August 2005

Abstract

The interaction of isotopic oxygen ($^{18}O_2$) with Zircaloy-4 (Zry-4) at 150 and 300 K has been studied using Auger electron spectroscopy (AES) and temperature-programmed desorption (TPD) methods. AES reveals the oxidation of the Zry-4 surface, reflected in shifts of the Zr(MNV) and Zr(MNN) features by about 5.5 and 3.0 eV, respectively, for both adsorption temperatures. The O(KLL)/Zr(MNN) Auger peak-to-peak height ratios as a function of exposure show the same trends at both temperatures. Following $^{18}O_2$ adsorption at 150 or 300 K, TPD experiments show hydrogen desorption near 400 K that is attributed to the presence of a surface-stabilized form of hydrogen. Additionally, water ($H_2{}^{18}O$ and $H_2{}^{16}O$) desorption below 200 K and above 700 K is observed after 150 K oxygen adsorption. However, after oxygen adsorption at 300 K the only significant desorption features are from isotopic water ($H_2{}^{18}O$). These findings indicate that mass transport involving the near-surface region contributes to the observed desorption, and that this behavior is dependent on the original adsorption temperature. Charging experiments using D_2 prior to and after $^{18}O_2$ adsorption were also performed and support our conclusions about the role of surface–subsurface mass transport in this system.

1. Introduction

The interaction of oxygen with zirconium surfaces has been extensively investigated in the past. However, there are only a few studies employing desorption techniques [1–5]. In an early study of oxygen on polycrystalline zirconium conducted by Foord et al. [2], following adsorption of oxygen no significant desorption of oxygen or oxygen-containing species was observed. Instead, rapid surface-to-bulk diffusion was reported. Asbury et al. [3] reported only hydrogen desorption following oxygen adsorption on polycrystalline zirconium. The desorption of hydrogen in the presence of surface oxygen was reported in another study as well [4]. In a report concerning the interaction of oxygen with Zircaloy-4 (Zry-4), desorption of hydrogen (D_2) was reported near 350 and 700 K [5]. However, none of these studies, except the one conducted previously in our laboratory on $^{18}O_2$/Zr(0001) [1], reported the desorption of water in temperature-programmed desorption (TPD) experiments.

Both theoretical [6,7] and experimental [8–10] studies indicate that subsurface adsorption (i.e. absorption) on zirconium dominates for oxygen at low exposures. It is known that annealing

* Corresponding author. Tel.: +1 330 972 4936; fax: +1 330 972 6918.
E-mail address: rex@uakron.edu (R.D. Ramsier).

0022-3115/$ - see front matter © 2005 Elsevier B.V. All rights reserved.
doi:10.1016/j.jnucmat.2005.08.022

zirconium, with oxygen present in the near-surface region, results in dissolution of oxygen atoms into the bulk rather than desorption. This is not surprising if one considers that the solid solubility of oxygen in zirconium can approach 30 at% [11]. Zirconium oxidation is of significant technological interest, and has been widely studied (see Ref. [11] and references therein, for example). In a study of room-temperature oxidation of Zircaloy-2 by oxygen [12], ZrO_2, Zr_2O, ZrO and Zr_2O_3 were found, with the formation of ZrO_2 near exposures of 0.3 L ($1.0\ \mathrm{L} = 1.33 \times 10^{-4}$ Pa s). In this present study, we are interested in comparing 300 K oxygen adsorption on Zry-4 with that at 150 K, to investigate the effects of adsorption temperature. Adsorption at 300 K is used for comparison to earlier studies, whereas 150 K adsorption may reveal physisorbed and/or weakly chemisorbed states and is, therefore, fundamentally important.

Comparing this work on Zry-4 with our previous studies of single crystal systems may answer open questions about the role of surface structure and alloying elements on Zr surface chemistry. In particular, the interaction of $^{18}O_2$ with Zr(0001) has previously been studied in the same ultra-high vacuum (UHV) system in our laboratory [1]. In that work, no desorption of oxygen was observed, consistent with other studies dealing with oxygen–zirconium interactions. However, unlike these other studies, the desorption of water from Zr(0001) was observed at high temperatures. In the data reported here from the $^{18}O_2$/Zry-4 system, we also observe the desorption of water. Isotopic mixing and mass transport contribute to the production of $H_2{}^{16}O$ and $H_2{}^{18}O$ in TPD experiments, consistent with our $^{18}O_2$/Zr(0001) study [1]. We additionally report the desorption of hydrogen at three temperatures: slightly above 400 K, near 720 K and above 750 K. Although our work is performed under UHV conditions, we provide further understanding of the kinetic processes of oxygen and hydrogen on Zry-4 surfaces. This makes our work relevant to studies dealing with the oxidation of Zry-4 under more realistic conditions found in nuclear engineering applications [13–15].

2. Experimental details

Experiments are performed in a stainless steel UHV system whose detailed description is given elsewhere [16,17]. During experiments, an ion getter pump in combination with a titanium sublimation pump was used. The vacuum chamber was pumped by a turbo-molecular pump (TMP) during 2 keV Ar^+ sputtering of the sample. The TMP was also used for pumping the gas-handling system prior to each oxygen exposure. The cleaning procedure consisted of sputtering (Ar, 99.9999%, Matheson), followed by annealing to 920 K. Annealing Zry-4 to this temperature does not induce sulfur segregation to the near surface region [18], whereas carbon and oxygen are almost completely dissolved into the bulk. The base pressure during experiments reported here was approximately 5×10^{-8} Pa.

The Zry-4 sample, cut from sheet stock provided by Wah Chang, has a thickness of 2 mm and a surface area of 0.53 cm^2. The sample was mechanically polished to a mirror-like finish with successively finer diamond pastes, and finally with a 0.05 μm alumina suspension. After polishing, the sample was placed in an ultrasonic bath for 20 min in a solution of Micro-90 (International Products Corp.), and then in acetone. Isotopic oxygen ($^{18}O_2$, min. 99%, Matheson) and deuterium (D_2, 99.7%, Matheson) are introduced from lecture bottles into the main chamber via a molecular beam doser described previously [19]. Auger electron spectroscopy (AES) is used to verify the cleanliness of the surface, based on our criteria that the O(KLL)/Zr(MNN) and C(KLL)/Zr(MNN) ratios are below 0.10.

Tantalum wires, spot-welded to the sample, are used for DC heating. Two type-E thermocouples, also spot-welded to the sample, are part of a temperature-control feedback loop. Sample cooling is performed by means of a copper braid connected to a liquid-nitrogen cold finger. Retarding-field AES with an electron beam energy of 3 keV is used. In the low-temperature experiments, we observe that the electron beam used for AES raises the temperature of the sample approximately 20 K during data collection. Therefore, for 150 K adsorption cases the Auger data collection was performed nominally at 170 K, whereas for 300 K adsorption experiments the temperature controller maintained the sample at 300 K during AES analysis.

3. Results and discussion

3.1. Auger electron spectroscopy

Fig. 1 shows a series of derivative-mode Auger spectra taken after oxygen adsorption at 150 K, indicating how zirconium Auger features change as a function of oxygen exposure. At about

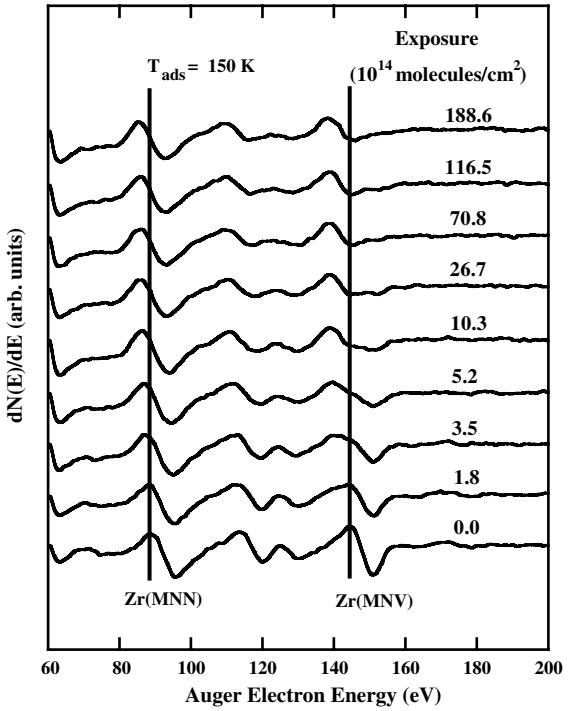

Fig. 1. Auger electron spectra of Zry-4 after different exposures to $^{18}O_2$ near 150 K. At high exposures, the Zr(MNV) feature shifts by 5.5 eV and changes shape, while the Zr(MNN) feature shifts by 3.0 eV.

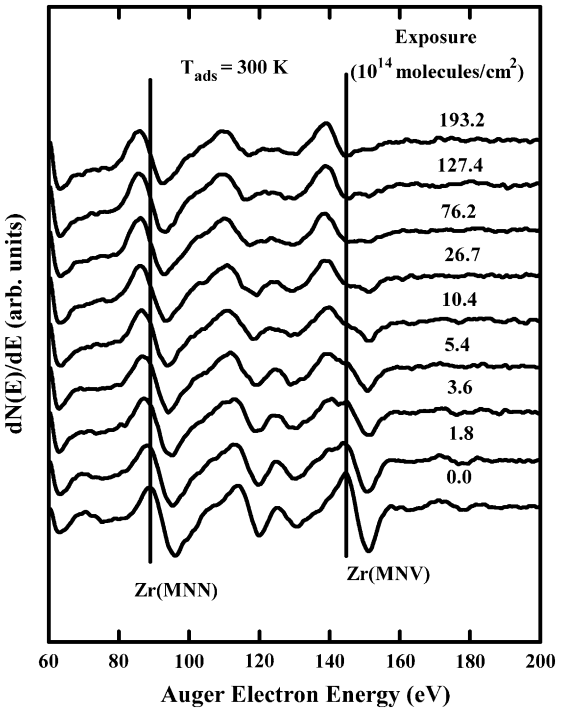

Fig. 2. Auger electron spectra of Zry-4 after different exposures to $^{18}O_2$ near 300 K. At high exposures, the Zr(MNV) feature shifts by 5.5 eV and changes shape, while the Zr(MNN) feature shifts by 3.0 eV.

3.5×10^{14} molecules/cm^2, the Zr(MNV) feature (which overlaps with the S(LMM) feature) shifts by about 5.5 eV and stays at the same position as exposure is increased further. The Zr(MNN) feature is less affected, and shifts by about 3.0 eV. The uncertainty in Auger electron energy shifts is about 0.5 eV. In a study of $^{18}O_2$ interaction with Zr(0 0 0 1) performed in our laboratory [1], the Zr(MNV) peak shift was only about 2 eV. However, that study was performed by backfilling the chamber, not with a line-of-sight gas doser. Note the changes in the shape of the Zr(MNV) feature. Initially, this feature changes significantly with exposure unlike the Zr(MNN) transition, and is apparently more sensitive to surface oxidation since it involves valence electrons. We therefore use the Zr(MNN) feature for calculating AES intensity ratios.

Low-temperature studies, in our case 150 K, are primarily of fundamental interest. Temperatures of applied interest are typically room temperature, or for nuclear applications 600–700 K [13–15]. In this article, we intend to compare low-temperature (150 K) oxygen adsorption with that at 300 K on this alloy. Fig. 2 shows how zirconium AES features change when oxygen is adsorbed at 300 K. It is interesting that oxygen adsorption at 300 K results in very similar Auger electron spectra to those obtained after adsorption at 150 K. Again, both Zr(MNV) and Zr(MNN) features shift with exposure by 5.5 and 3.0 eV respectively, with the Zr(MNV) feature undergoing significant line shape changes.

Fig. 3 shows how zirconium AES features change after exposure to $^{18}O_2$ at 150 K and subsequent annealing, whereas Fig. 4 shows a similar series of AES measurements taken after exposure to $^{18}O_2$ at 300 K. In both sets of measurements, the oxygen exposure was 76.6×10^{14} molecules/cm^2. The same conclusions can be drawn for both adsorption temperatures. The oxide layer that forms on the surface of Zry-4, consistent with observations on polycrystalline zirconium [20], disappears above 650 K. Where the oxygen goes – dissolution into the bulk or desorption from the surface – will be discussed in the next section. Our use of isotopic oxygen, although not necessary for the AES studies reported in this section, will allow us to identify mass transport and mixing phenomena in TPD.

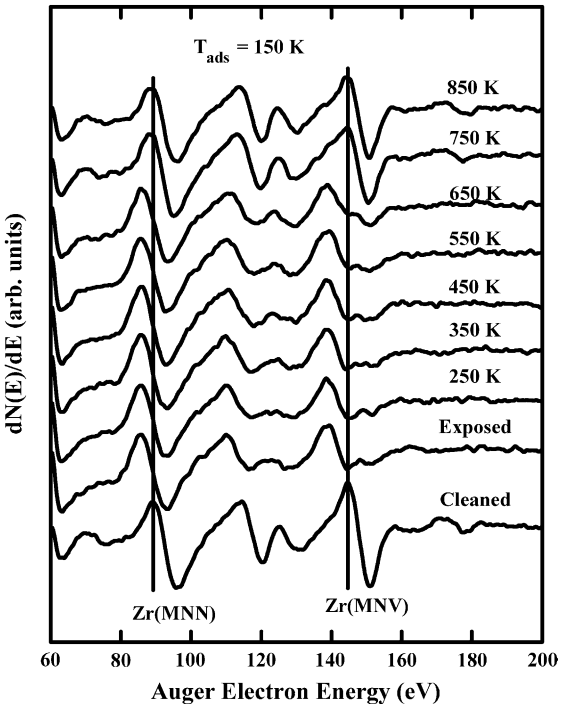

Fig. 3. Auger electron spectra of Zry-4 upon cleaning, $^{18}O_2$ exposure at 150 K, and stepwise annealing.

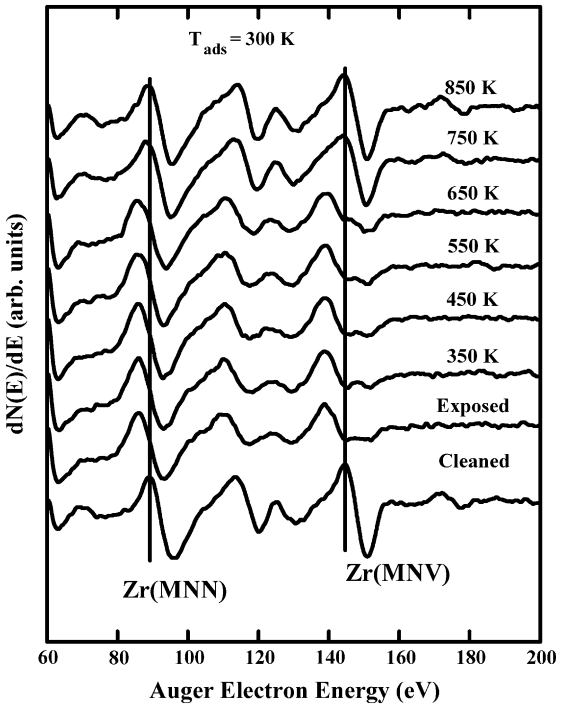

Fig. 4. Auger electron spectra of Zry-4 upon cleaning, $^{18}O_2$ exposure at 300 K, and stepwise annealing.

Fig. 5 shows the O(KLL)/Zr(MNN) ratios versus oxygen exposure at the two temperatures studied here. Solid points represent oxygen adsorption at 150 K whereas hollow points correspond to adsorption at 300 K. The Zr(MNN) signal intensity does not vary significantly with oxygen exposure (see for example Figs. 1 and 2), so the O(KLL)/Zr(MNN) ratio reflects, to a good approximation, the oxygen content in the near-surface region. It is evident that an exposure of approximately 100.0×10^{14} molecules/cm^2 results in oxygen saturation in both cases. Moreover, both data sets show the same trend and are difficult to distinguish, consistent with the fact that the sticking coefficient of oxygen on zirconium is approximately unity for a wide range of temperatures, up to one monolayer [21]. We detect no significant difference in the uptake of oxygen even at higher exposures. Note that our exposures would extend the surface coverage beyond one monolayer, if the sticking coefficient is constant.

We see no difference in the amount of near-surface oxygen on Zry-4 following adsorption at 150 or 300 K, consistent with the Auger spectra of the Zr features shown in Figs. 1–4, which exhibit similar trends for both adsorption temperatures. We point out that in our experiments, after dosing, the position of the sample has to be changed for AES measurements. Even though care has been taken to place the sample and the beam doser in the same positions each time, it is possible that different surface regions have been analyzed. This will add to the uncertainty in our AES measurements, as will electron beam damage effects.

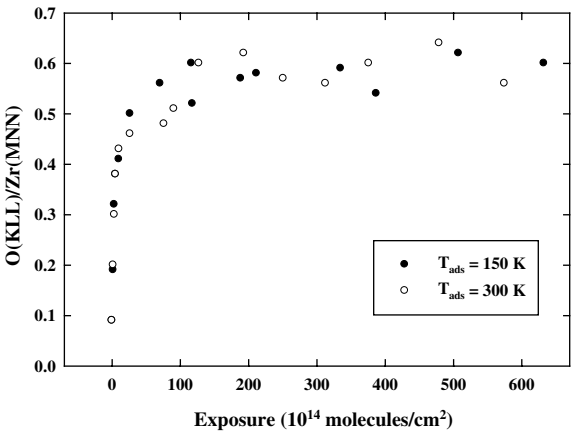

Fig. 5. Dependence of the ratio of the O(KLL) to Zr(MNN) Auger peak-to-peak heights at adsorption temperatures of 150 K and 300 K. An exposure of about 100×10^{14} molecules/cm^2 results in oxygen saturation for both adsorption temperatures.

3.2. Temperature-programmed desorption

In Figs. 6 and 7 we compare isotopic water ($H_2{}^{18}O$) desorption features after oxygen adsorption at 150 and 300 K, respectively. The same exposure sequence is used and shown in both figures. Since no desorption of molecular oxygen has been observed in TPD experiments after O_2 adsorption in this study, we conclude that dissociation of adsorbed molecules takes place at temperatures as low as 150 K. Oxygen typically diffuses into the bulk of Zr upon high-temperature annealing, and our low exposure data are consistent with this. However, since we observe the desorption of $H_2{}^{18}O$ we propose that high oxygen exposures saturate the near-surface region and open another pathway for the removal of oxygen. Instead of diffusion into the bulk, some of the oxygen undergoes reaction with hydrogen to desorb as water. Relatively poor signal-to-noise in our TPD spectra indicate that the amount of desorbing water is relatively small and is, therefore, mostly relevant from a fundamental rather than an applied point of view.

Comparing Figs. 6 and 7, we see that the TPD profiles for $H_2{}^{18}O$ desorption following $^{18}O_2$ adsorption at 300 K are different from those following 150 K adsorption. Also, even though the signal intensity is expressed in arbitrary units, the vertical scale is the same in these figures to indicate the relative amounts of desorbing molecules. Calculating the integrated areas, which are proportional to the number of desorbing molecules, we find that about three times more isotopic water desorbs following adsorption at 150 K. Also, for the highest exposure shown, approximately five times more water is detected in the low temperature peak following 150 K adsorption. Note that this low-temperature peak following 300 K adsorption is shifted toward 200 K and does not have a well-defined shape.

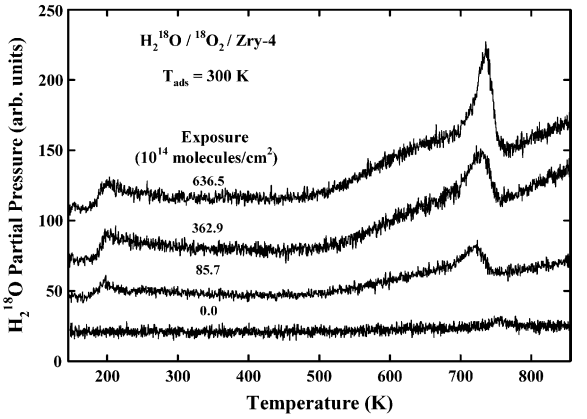

Fig. 7. Temperature-programmed desorption of isotopic water ($H_2{}^{18}O$) after different exposures to $^{18}O_2$ at 300 K.

Figs. 8 and 9 show TPD spectra of normal water ($H_2{}^{16}O$) following $^{18}O_2$ adsorption at 150 and 300 K, respectively. The spectra are from the same experiments as those in Figs. 6 and 7. This time, the differences in TPD profiles and yields are even more significant. After $^{18}O_2$ adsorption at 300 K, the low-temperature desorption feature is slightly shifted toward higher temperatures and is significantly reduced, and the high-temperature feature is almost completely absent. Even though AES data show basically no difference between adsorption at these two temperatures, TPD results distinguish between the two systems. Similar to what Figs. 6 and 7 indicate,

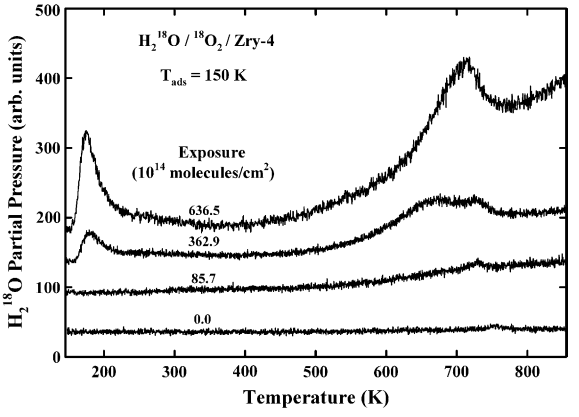

Fig. 6. Temperature-programmed desorption spectra of isotopic water ($H_2{}^{18}O$) after different exposures to $^{18}O_2$ at 150 K.

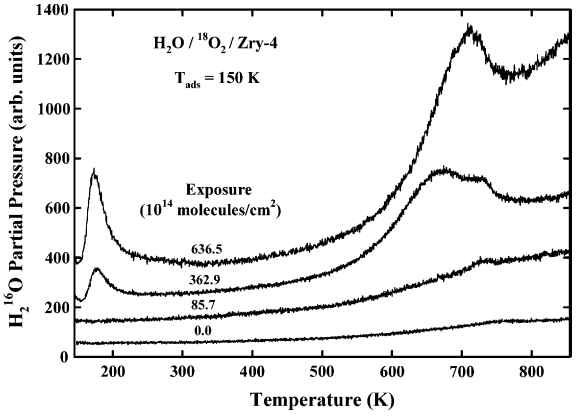

Fig. 8. Temperature-programmed desorption of regular water ($H_2{}^{16}O$) after different exposures to $^{18}O_2$ at 150 K.

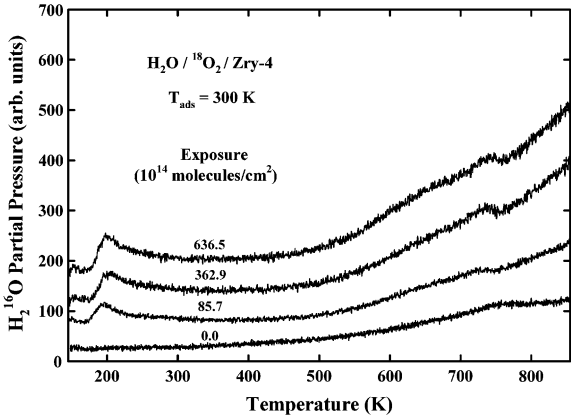

Fig. 9. Temperature-programmed desorption of regular water ($H_2{}^{16}O$) after different exposures to $^{18}O_2$ at 300 K.

poor signal-to-noise in these spectra reveal that the amount of desorbing water is relatively small.

The use of isotopic oxygen allows us to propose that temperature-dependent mixing of oxygen species adsorbed from the gas phase with those already present in the Zry-4 sample occurs. Comparing Figs. 6 and 8, we see that for 150 K adsorption more normal water desorbs in both the low and high temperature states than isotopically labeled water. However, a comparison of Figs. 7 and 9 indicates that only isotopic water exhibits a well-defined desorption state, and only at high temperature. It is not surprising to have more 200 K desorption following adsorption at 150 K versus 300 K. We propose that oxygen dissociates on Zry-4 even at 150 K, and that hydrogen is attracted from the near-surface region (surface or subsurface) to the O-covered surface even at low temperatures, desorbing as water during heating near 200 K. This process occurs with the oxide layer still intact, whereas the high-temperature desorption starts before the oxide layer has begun to dissolve. Thus, the mass transport resulting in the low- and high-temperature desorption states of water occur under different conditions.

The exact mechanism for the desorption of water in the high temperature state is not known. Since hydrogen is known to segregate from the bulk and rapidly desorb above 700 K in vacuum [22,23], we cannot rule out that, on its way to the surface, hydrogen interacts with mobile oxygen and then hydroxyl species and combines to desorb as water. It is also worth mentioning that oxygen was found to induce segregation of bulk hydrogen to the surface [24], which could be the case in our experiments also. However, the high-temperature desorption that we observe in TPD starts before removal of the oxide layer as indicated by AES making the interpretation of our results even more difficult. Our recent results of H_2O adsorption on Zry-4 at 150 K clearly show that hydrogen from dissociated water plays an important role in the formation of water at high temperatures [25]. Surface hydrogen, always present on this gettering material, may be involved in water production. We rule out significant background contamination since we do not observe water desorption peaks when the sample is exposed to background gases for time intervals longer than those used in these experiments.

We propose that at higher exposures, the subsurface region saturates with oxygen which delays or blocks the diffusion of near-surface or surface oxygen into the bulk. This consequently opens a new channel for near-surface oxygen; desorption as water. Comparing isotopic and regular water desorption for 150 K adsorption, we find that approximately four times more regular water desorbs for this temperature. However, following $^{18}O_2$ adsorption at 300 K regular water does not exhibit well-defined desorption features. This is interesting, and is not a result of background contamination. The implication is that isotopic mixing and mass transport of oxygen occur in Zry-4 even at 150 K.

Another finding of this work that deserves attention is the desorption of hydrogen induced by oxygen adsorption. Fig. 10 shows hydrogen TPD profiles without exposure (A) and following exposure to 493.2×10^{14} oxygen molecules/cm^2 at 300 K (B) and 150 K (C). Following adsorption of $^{18}O_2$ on Zry-4, three hydrogen desorption states are observed. Rapid H_2 desorption above 750 K is a result of segregation of bulk hydrogen to the surface and does not require oxygen. Based on the cracking fragment ratios we find the feature slightly above 720 K is not just a cracking fragment of desorbing water molecules. Instead, the formation of two species, molecular hydrogen and water, occurs at this temperature. Desorption slightly above 400 K is a direct consequence of adsorbed oxygen. Note that more hydrogen desorbs following 150 K adsorption.

Interaction between oxygen and hydrogen in zirconium-based materials is of interest for nuclear applications. There are several previous reports relevant to the work presented here concerning oxygen–hydrogen interactions. It has been reported that adsorbed oxygen induces segregation of bulk

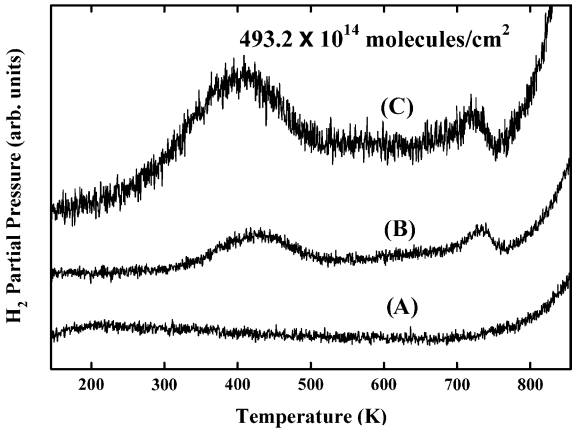

Fig. 10. Hydrogen TPD profiles without oxygen exposure (A) and following exposure to 493.2×10^{14} molecules/cm^2 at 300 K (B) and 150 K (C).

hydrogen to the surface [24]. In another study of oxygen–hydrogen interactions on polycrystalline zirconium, direct bonding of hydrogen to oxygen and Zr were identified employing TPD and electron-stimulated desorption methods [3]. The presence of an oxide layer retards hydrogen adsorption from the gas phase and also attracts hydrogen from the bulk to form a hydroxylated oxide layer on the surface.

Peterson et al. [4] reported a binding state for hydrogen on polycrystalline zirconium that had a desorption temperature of 500 K. This occurred in the presence of oxygen, presumably involving hydroxyl groups. They proposed that the surface oxygen attracts hydrogen from the metal. We observe in the present $^{18}O_2$/Zry-4 study that hydrogen desorption occurs slightly above 400 K. However, the heating rate in Ref. [4] was approximately 35 K/s as compared to our 1.8 K/s, which may explain the difference in these desorption temperatures. The hydrogen feature that we observe at about 720 K was not present in this previous study [4]. We note here that we have not heated our Zry-4 sample above the 1135 K phase-transition temperature, and that we also have to consider the possible role that alloying elements may be having on the migration and recombinative desorption of species during heating. However, the presence of tin in the near-surface region is not significant [18], and most likely not crucial for interpretation of our results. All other alloying elements are at the edge or below our AES detection limits.

The origin of the hydrogen that participates in water desorption is an open question. Charging experiments using D_2 and $^{18}O_2$ were performed to address this. Interestingly, no desorption of D_2 is observed even in experiments that involved charging of the sample with deuterium both prior to and after $^{18}O_2$ adsorption. The fact that we do not observe the desorption of molecular deuterium when the sample is pre-dosed with oxygen is consistent with a previous study by Asbury et al. [3], who reported that an oxygen-covered zirconium surface prevents subsequent hydrogen adsorption [3]. Asbury et al. also proposed that when zirconium is exposed to deuterium most of the D is absorbed to bond to zirconium atoms. Subsequent oxygen adsorption results in attraction of regular hydrogen from the near-surface region rather than the dissolved deuterium, which diffuses more slowly.

Fig. 11 shows TPD spectra of the 20 amu water signal after 150 K exposure to D_2 (600.0×10^{14} molecules/cm^2) and $^{18}O_2$ (400.0×10^{14} molecules/cm^2). Note that the water desorption features are more pronounced when the sample was charged with isotopic oxygen first. Since it is known from the literature that oxygen-covered zirconium prevents deuterium adsorption [3], it is evident that this 20 amu QMS signal originates from $H_2{}^{18}O$ rather than $D_2{}^{16}O$ water. This assignment was also verified by examining the cracking fragment ratios.

The reason that we propose for the reduction in the water desorption features when the sample was

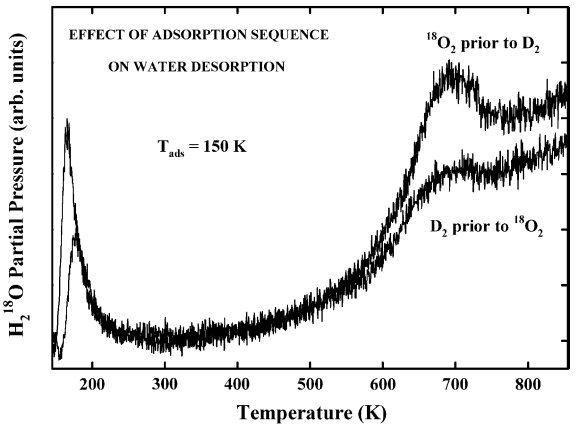

Fig. 11. Temperature-programmed desorption of isotopic water (20 amu) after charging experiments at 150 K. Smaller water features are evident when the sample is charged with D_2 (600.0×10^{14} molecules/cm^2) first and then exposed to $^{18}O_2$ (400.0×10^{14} molecules/cm^2), versus the opposite sequence. The other cracking fragments (not shown) indicate that the 20 amu signal originates from $H_2{}^{18}O$ rather than $D_2{}^{16}O$, and thus that the hydrogen involved in the formation of water originates from the Zry-4 substrate.

first charged with D_2 is that during deuterium absorption the H/D ratio near the surface is reduced. Therefore, fewer hydrogen atoms are available to combine with oxygen to desorb as water. This is a diffusion-controlled reaction, with competition between oxygen dissolution into the sub-surface and hydrogen migration out of the sub-surface. In our model, deuterium adsorbed before oxygen is not recovered, but dissolves into the bulk. However, it limits the outward diffusion of H, resulting in decreased water production. Note that our charging experiments (in the range of 10^{16} molecules) involve at least an order of magnitude fewer deuterium atoms than would be necessary to achieve even ppm bulk concentrations.

Conversely, deuterium exposures after oxygen adsorption do not result in D adsorption or ingress, thus the production of water is not affected. Note that this latter point indicates that H adsorption from the background gases onto the oxygen-covered substrate cannot be responsible for the production of water. Otherwise, we would have detected D_2O. Rather, the hydrogen observed in TPD must originate from the near-surface region of Zry-4. Of course, the amount of hydrogen within the bulk is finite. This would be replenished by the gettering of background gases from the chamber by Zry-4 upon cooling after a TPD ramp. Therefore, the ultimate origin of the H that combines to form water in our experiments is the background gases, but the water is actually formed from outward-migrating H that combines with oxygen at the surface and desorbs during heating.

4. Conclusions

This UHV study of the adsorption of oxygen ($^{18}O_2$) on Zry-4 at 150 and 300 K reveals surface oxidation with similar behavior at both temperatures. The Zr(MNV) feature changes shape as a function of exposure and, for higher exposures, shifts by about 5.5 eV. The Zr(MNN) does not change shape significantly but shifts by about 3.0 eV. AES shows no significant difference for the two temperatures studied here. Also, $^{18}O_2$ presumably dissociates at both adsorption temperatures, since we do not observe the desorption of molecular oxygen. For low exposures, heating the substrate to high temperatures results in oxygen dissolution into the bulk. For higher exposures, the subsurface region saturates with oxygen. Heating the sample then results in the desorption of water below or near 200 K and above 700 K. We propose that oxygen from the surface or near-surface region undergoes reaction with outward-segregating hydrogen to desorb in the form of water.

Acknowledgements

Acknowledgement is made to the Donors of the American Chemical Society Petroleum Research Fund for partial support of this research. We would also like to thank Wah Chang for providing the Zry-4 material. In addition, we would like to thank the anonymous referees who raised good questions and helped us to improve this manuscript.

References

[1] Y.C. Kang, R.D. Ramsier, Appl. Surf. Sci. 195 (2002) 196.
[2] J.S. Foord, P.J. Goddard, R.M. Lambert, Surf. Sci. 94 (1980) 339.
[3] D.A. Asbury, G.B. Hoflund, W.J. Peterson, R.E. Gilbert, R.A. Outlaw, Surf. Sci. 185 (1987) 213.
[4] W.J. Peterson, R.E. Gilbert, G.B. Hoflund, Appl. Surf. Sci. 24 (1985) 121.
[5] N. Haruo, K. Chiken, H. Masahiro, Kogaku Shuho-Kyushu Daigaku 70 (6) (1997) 569.
[6] M. Yamamoto, C.T. Chan, K.M. Ho, S. Naito, Phys. Rev. B 54 (1996) 14111.
[7] G. Jomard, T. Petit, L. Magaud, A. Pasturel, G. Kresse, J. Hafner, Mol. Simul. 24 (2000) 111.
[8] C.-S. Zhang, B.J. Flinn, I.V. Mitchell, P.R. Norton, Surf. Sci. 245 (1991) 373.
[9] Y.M. Wang, Y.S. Li, K.A.R. Mitchell, Surf. Sci. 342 (1995) 272.
[10] Y.M. Wang, Y.S. Li, K.A.R. Mitchell, Surf. Sci. 343 (1995) L1167.
[11] T. Tanabe, M. Tomita, Surf. Sci. 222 (1989) 84.
[12] Y. Nishino, A.R. Krauss, Y. Lin, D.M. Gruen, J. Nucl. Mater. 228 (1996) 346.
[13] E.A. Garcia, G. Beranger, J. Nucl. Mater. 273 (1999) 221.
[14] H.S. Hong, S.J. Kim, K.S. Lee, J. Nucl. Mater. 273 (1999) 177.
[15] A. Grandjean, Y. Serruys, J. Nucl. Mater. 273 (1999) 111.
[16] Y.C. Kang, M.M. Milovancev, D.A. Clauss, M.A. Lange, R.D. Ramsier, J. Nucl. Mater. 281 (2000) 57.
[17] Y.C. Kang, R.D. Ramsier, J. Nucl. Mater. 303 (2002) 125.
[18] N. Stojilovic, E.T. Bender, R.D. Ramsier, Appl. Surf. Sci., in press.
[19] N. Stojilovic, J.C. Tokash, R.D. Ramsier, Surf. Sci. 565 (2004) 243.
[20] P.E. West, P.M. George, J. Vac. Sci. Technol. A 5 (1987) 1124.
[21] C.-S. Zhang, B.J. Flinn, P.R. Norton, Surf. Sci. 264 (1992) 1.
[22] J.-M. Lin, R.E. Gilbert, Appl. Surf. Sci. 18 (1984) 315.
[23] N. Stojilovic, R.D. Ramsier, Chem. Phys. Lett. 399 (2004) 53.
[24] K. Ojima, K. Ueda, Appl. Surf. Sci. 165 (2000) 149.
[25] N. Stojilovic, R.D. Ramsier, Appl. Surf. Sci., in press.